Slope stability assessment of the recent Birik Dara landslide in the Kalimpong region of Darjeeling Himalaya, India

Suvam Das[1,2], Prachi Chandna[1,2], Shantanu Sarkar[1,2,*] and Debi Prasanna Kanungo[1,2]

[1]Academy of Scientific and Innovative Research, Ghaziabad 201 002, India
[2]CSIR-Central Building Research Institute, Roorkee 247 667, India

The Birik Dara landslide occurred at around 10 pm local time (GMT+5:30) on 20 October 2021 on National Highway-10 in the Kalimpong region of Darjeeling Himalaya, India, and disrupted traffic for more than a week. This study presents an overview of the landslide and reveals the present stability status of the slope. The slope stability assessment was carried out using data collected from the field during a site visit in the second week of November 2021. The findings of this study indicate that the landslide occurred on a critically unstable slope and it may be triggered again in the near future with more damage. Therefore, immediate attention is required regarding slope stabilization measures to avoid future threats.

Keywords: Failure mechanism, hazard mitigation, landslide, rock mass, slope stability.

CONSIDERING different geological hazards, landslides being an open problem in hills and mountains cause loss of life and property. Though landslides are destructive, they are often overlooked and underestimated. They tend to be more disastrous and regime global attention to avoid perilous conditions. The vulnerability of landslides increases, particularly when they block the natural drainage by forming landslide dams, or may occur near roads and settlements. Therefore, in terms of risk, the landslide location is more significant than its size. A landslide occurred near Birik Dara in Kalimpong region of West Bengal, India. Named as Birik Dara landslide by the locals, it occurred on 20 October 2021 at 10 pm and washed away about 70 m road stretch of National Highway-10 (NH-10). This road is the major motorable route connecting Siliguri with Sikkim and Kalimpong, and has long been a major gateway for people living in this remote corridor. Due to this landslide, the road was blocked for more than a week and traffic was disrupted. Fortunately, no lives were lost. Prior to this landslide event, four consecutive extreme rainfall days were recorded at Teesta Low Dam-IV Power Station (TLD-IV PS) and the cumulative rainfall was 664.4 mm. Such antecedent rainfall plays an important role in initiating landslides by increasing the pore water pressure on the subsurface. This landslide was characterized as a shallow retrogressive rock-cum-debris slide and witnessed frequent occurrences in a short period. In 2021, the active portion of this landslide had extended towards the Teesta River and is now progressing retrogressively to the uphill slope section above the road. This landslide requires special attention because of its disastrous effect on NH-10 and the associated economic loss to the affected area. In this regard, the present study aims to describe the factors responsible for the Birik Dara landslide and estimates the stability coefficient of the present slope based on the data collected during the field survey.

The Birik Dara landslide occurred around 10 pm local time (GMT+5:30) on 20 October 2021, at 26°58′1.91″N and 88°25′38.92″E between Rambi and Kalijhora, at an elevation of about 304 m amsl, with slope direction N316° (Figure 1). Figure 2 shows photographs of the road condition after the hazard, while Figure 3 shows field photographs of the landslide. In 2021, the main scarp of this landslide was positioned over a convex slope of height around 50 m above road level with a slope inclination of 76°. The site visit revealed that this landslide was typically characterized as a rock-cum-debris slide with a visible head scarp and flanks on the upper slope section. Above the crown, vegetation cover was present with a thin soil layer of about 1.5 m. The displaced materials accumulated below the road are mainly comprised of boulders and rock fragments with soil mass (Figure 3). The crown and toe of this landslide were at a distance of about 200 m with an elevation of 360 and 223 m respectively. The depth (D_d), width (W_d) and length (L_d) of the displaced mass were approximately 3, 60 and 150 m respectively. After initiation, the landslide damaged NH-10 and moved downhill towards the Teesta River. On the right flank, a small drainage channel was found, that may have increased the relative erosion rate and in turn the volume of debris during sliding. The estimated volume of the entire landslide body ($\pi \times L_d \times D_d \times W_d/6$) was roughly 14,137 m^3 (ref. 1). The temporal Google Earth images depict the shifting and enlargement of this landslide body from its actual path during 2016–2020 (Figure 4 *a*) and indicates high temporal recurrence probability. The exact date of events prior to 2021 is unavailable in the historical database and by interviewing the local residents it was learned that past events at this location did not cause any damages. On 20 October 2021, this landslide was reactivated by consecutive heavy rainfall events for a few days. A spatial comparison of this landslide based on Google Earth images reveals that the main scarp was located below the road level having a total length of about 140 m during 2020, and thereafter, the slope above the road failed in 2021. Such recurrence with uphill expansion emphasizes the retrogressive nature of the Birik Dara landslide. Figure 4 *b* shows the schematic cross-sectional representation of this landslide and advocates that its position is the most dominating aspect regarding its risk.

*For correspondence. (e-mail: shantanu_cbri@yahoo.co.in)

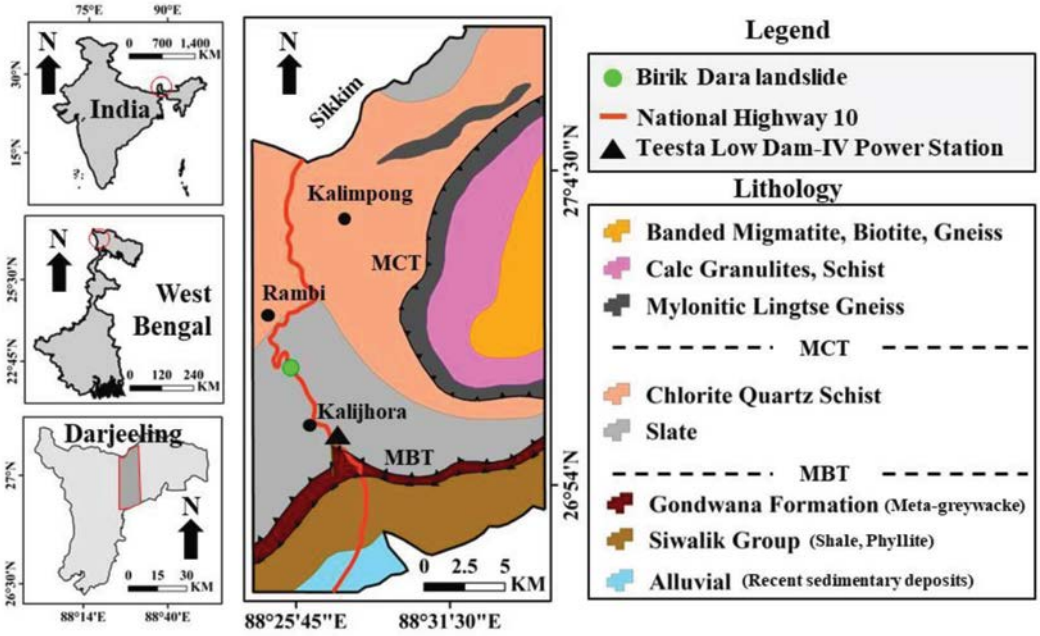

Figure 1. Location map of the Birik Dara landslide with the regional lithology (after Acharyya[2] and Das *et al.*[11]).

Figure 2. Road condition after the landslide. (Source: Fastest Fast Sikkim YouTube channel and *East Mojo* newspaper.)

Geologically, the study area is underlain by the Daling series rock types, including meta-greywacke, slate, chlorite quartz schist and phyllite rocks (Figure 1)[2]. The site visit also revealed the presence of similar rock types in this area. The terrain consisted of rugged mountains running in all directions, separated by drainage valleys. Site inspection of this landslide indicated that the failure area mainly extended along a small folded ridge with steep terrain in the southeast and low in the northwest directions towards Teesta River. The typical association of different rock strata in the sliding zone reveals the complex geological attribute of this area and its proximity to the MBT (Main Boundary Thrust) also strengthens the seismic vulnerability. Phyllite and slate are the dominant rock types present in the sliding zone (Figure 3). These rocks are highly weathered and sheared, and easily disintegrated by hand. Considering the degree of rock mass weathering proposed by Goel *et al.*[3], the identified rocks were categorized as grade IV to grade V classes. Discontinuities and closely spaced joint sets were visible in the main scarp area (Figure 3). The general dip direction of the prominent joint set was towards the northwest (N302°) with a dip of 68°. Table 1 presents a detailed description of the slope and joints. The geological evaluation reveals that the present study area has been subjected to intense tectonic activities in the geologic past and endorses the fact that the area is highly susceptible to landslides. Therefore, geological characteristics are considered one of the major preparatory factors for landslide occurrences in this area. During the field survey, representative rock samples were collected from the sliding surface, namely locations L1–L4 (Figure 3) for characterizing the engineering and physical properties.

In the present study, daily rainfall data (mm/day) during the past 20 years (3 November 2002–2021) were collected from TLD-IV PS, located about 5 km southeast of the landslide site (Figure 1). The data show that the area received an average annual rainfall of about 3748.86 mm, with a unimodal peak during June–August (Figure 5 *a*). Figure 5 *b* shows rainfall data in October 2021. Critical analysis of the date of initiation in relation to the period of rainfall revealed that delayed monsoon rainfall had a pronounced effect on this landslide. On 20 October 2021, the landslide was triggered after an episode of extreme rainfall events for four days (87.6, 182.4, 209.2 and 160.8 mm of rainfall on 16, 17, 18 and 19 October 2021 respectively) that may have developed successive wetting fronts as well as increased pore pressure, thereby decreasing the shear strength of the highly weathered slope materials. Thus, it indicates that

Figure 3. Field photographs of Birik Dara landslide. L1–L4 represent locations from where rock samples were collected for laboratory testing.

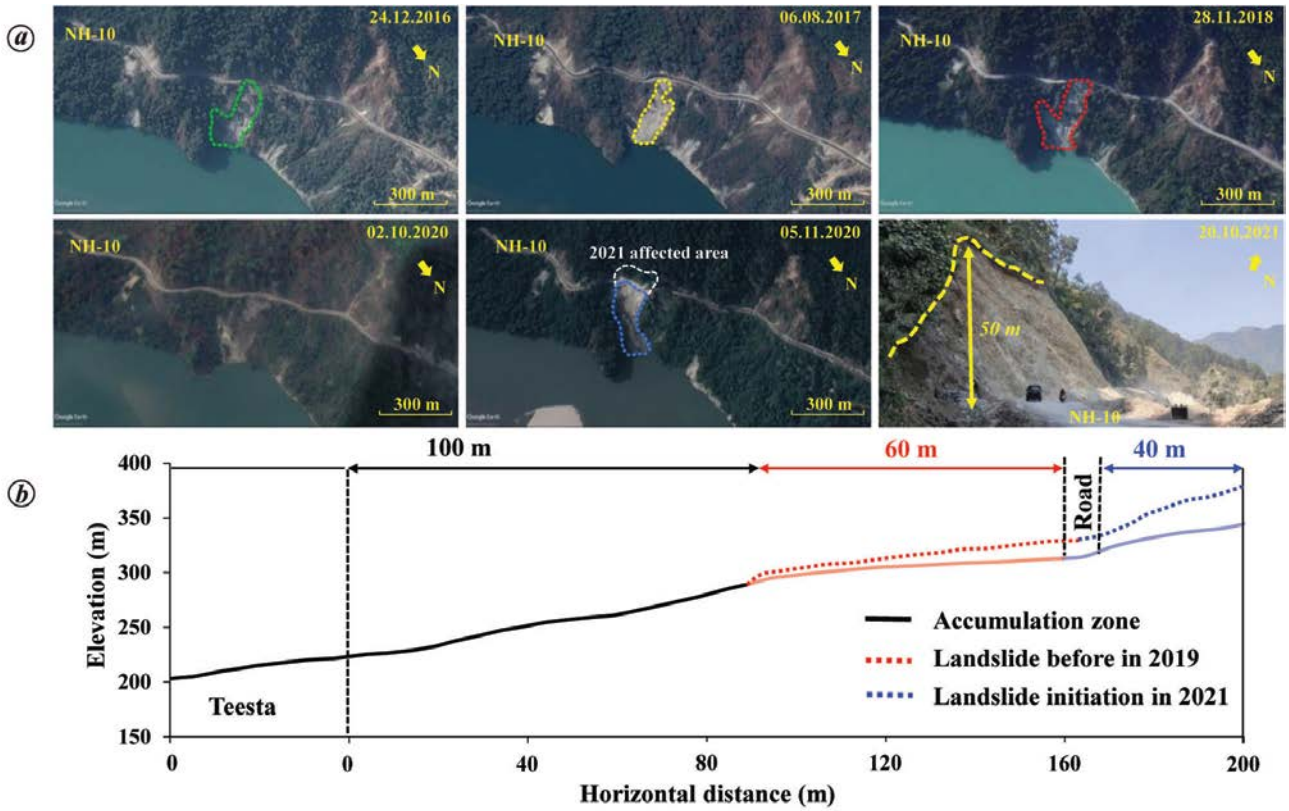

Figure 4. ***a***, Temporal Google Earth (® Google Inc.) images of Birik Dara landslide. ***b***, Schematic cross-sectional representation of the landslide.

Table 1. Description of the discontinuities observed in the exposed rock mass

	Joint orientation		
Slope orientation	J1	J2	J3
N316°/76°	N302°/68°	N144°/46°	N218°/38°

high-intensity rainfall was responsible for triggering the Birik Dara landslide.

Considering this scenario, we used different empirical techniques (kinematic analysis, rock mass rating, slope mass rating, geological strength index) and numerical modelling (finite element modelling) to precisely gauge the stability

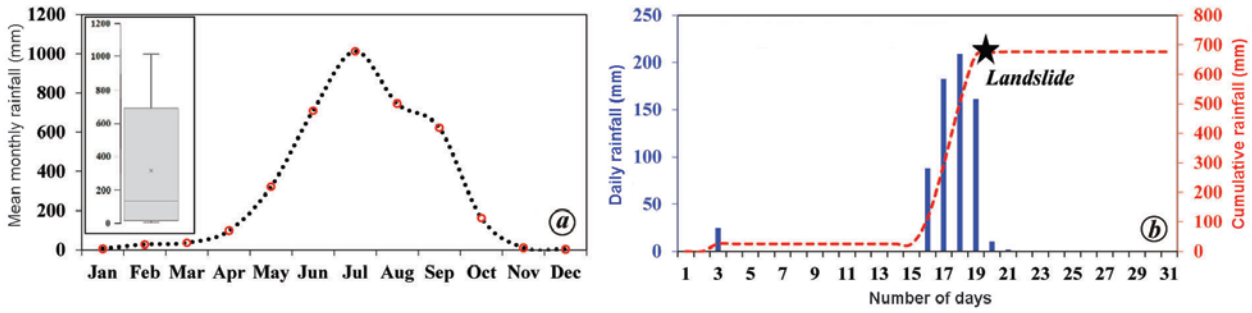

Figure 5. ***a***, Mean monthly rainfall for the past 20 years (3 November 2002–2021). ***b***, Daily recoded rainfall during October 2021.

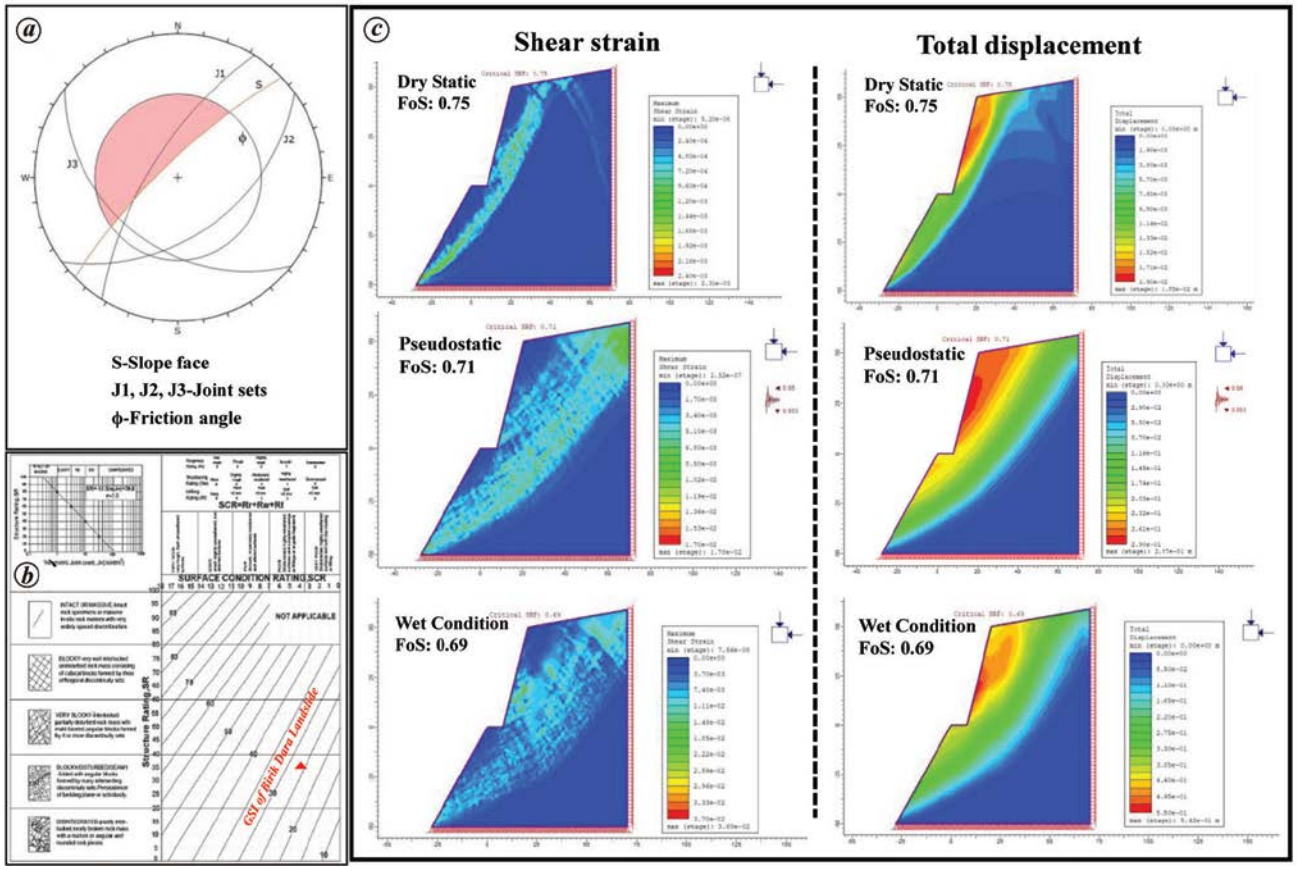

Figure 6. ***a***, Kinematic analysis showing the joints–slope relationship. ***b***, GSI chart showing the quantified GSI value of the studied slope (after Sonmez and Ulusay[10]). ***c***, FEM-based stability analysis of the slope section.

of the present slope. A detailed description is presented below.

Kinematic analysis was carried out using the Markland's test described by Hoek and Bray[4] to interpret the slope–joints relationship. Table 1 presents the geometric orientation of the slope face (S) and the three identified joint sets (J1–J3) and in Figure 6 *a*, these are plotted in a stereographic projection. Notably, the structural orientation of J1 and slope face satisfies the conditions of a critical plane (dip direction ±20°) and justifies J1 offering a planar mode of failure for the landslide that occurred in 2021.

According to the rock mass rating (RMR) system proposed by Bieniawski[5], five parameters, namely unconfined compressive strength (UCS), rock quality designation (RQD)[6], joint spacing, joint condition and hydrological condition, have been evaluated to determine the basic RMR (RMR_{basic}). To determine UCS, a few rock samples collected during the field survey were tested in the laboratory using a point load testing machine. Thereafter, based on the site visit, RMR ratings were assigned to all parameters and their arithmetic sum gave an RMR_{basic} value of 39. Table 2 presents a detailed description of these parameters and their assigned ratings.

The slope mass rating (SMR) system of Romana[7] is a commonly used empirical method to estimate the stability likelihood of both natural and cut slopes. The SMR technique is

frequently used to assess slope stability in the Indian Himalayan region, particularly along the hill roads[8]. SMR can be calculated using as follows

$$\text{SMR} = \text{RMR}_{\text{basic}} + (F_1 \cdot F_2 \cdot F_3) + F_4, \quad (1)$$

where F_1 measures the parallelism between slope face and joint plane or the plunge line (intersection line of two joint sets) orientation. F_2 depends on the dip amount of the joint plane or the plunge line. F_3 depends on the relationship between dip of the slope and dip of the joint plane or the plunge line. F_4 is the adjustment factor which depends on the method of excavation. For the present study, the adjustment ratings of F_1, F_2, F_3 and F_4 have been defined following the SMR scheme of Romana[7] (Table 2). The calculated SMR was found to be 19 for the present slope, indicating a completely precarious condition.

The geological strength index (GSI) proposed by Hoek and Brown[9] estimates the strength and deformation characteristics of rock masses with respect to the blockiness and joint condition. For this study, the GSI chart given by Sonmez and Ulusay[10] was used to define the quantitative GSI value. This chart helps practitioners avoid inadvertent errors and inconsistencies during rock mass classification compared to the GSI chart proposed by Hoek and Brown[9]. Two empirical equations (eqs (2) and (3)), namely structural rating (SR) and surface condition rating (SCR), were suggested by Sonmez and Ulusay[10] to define the GSI value. They are as follows

$$\text{SR} = -17.5 \ln(J_v) + 79.8, \quad (2)$$

$$\text{SCR} = R_r + R_w + R_i, \quad (3)$$

where J_v is the volumetric joint count ($J_v = 1/S_1 + 1/S_2 + 1/S_3 \ldots + 1/S_n$, where S_1, S_2, S_3 and S_n are the average joint spacing). The SR and SCR values obtained were 32.41 and 4 respectively (Table 2). Thus, the GSI value obtained for the studied slope was 27 (Figure 6 *b*). The low value of GSI indicates that the rock mass quality of the slope is poor and such slopes are often susceptible to landslides.

Further to quantify the slope stability, a finite element modelling (FEM) program in RS[2] software was utilized. Here, the shear strength reduction (SSR) technique was adopted for FEM-based slope stability analysis considering the physical and engineering properties of the slope-forming material. SSR technique determines the strength reduction factor (SRF) following static (gravity loading) and pseudo-static (to simulate earthquake behaviour) conditions and estimates the factor of safety (FoS) value. Generally, FoS is the ratio between the shear strength (resisting force) of the slope-forming material and the shear stress (driving force). If FoS < 1, the slope is considered as unstable, while higher FoS values (≥1) signify a more stable slope. Thus, the strength behaviour of the rock mass is important to assess SRF. In this study, the generalized Hoek–Brown (GHB) strength criterion was utilized to assess the strength behaviour, and the Hoek–Brown parameters (m_b, s and α) were determined from the GSI value of the slope. Equations (4) to (7) define the GHB criteria.

$$\sigma_1 = \sigma_3 + \sigma_{ci}\left(\frac{m_b\sigma_3}{\sigma_{ci}} + s\right)^{\alpha}, \quad (4)$$

$$m_b = \exp\left(\frac{\text{GSI} - 100}{28 - 14D}\right) m_i, \quad (5)$$

$$s = \exp\left(\frac{\text{GSI} - 100}{9 - 3D}\right), \quad (6)$$

$$\alpha = 0.5 + \frac{1}{6}\left[\exp\left(-\frac{\text{GSI}}{15}\right) - \exp\left(-\frac{20}{3}\right)\right], \quad (7)$$

where σ_1 and σ_3 are the major and minor principal stress respectively; σ_{ci} represents the uniaxial compressive strength of the intact rock; m_b, s and α are the empirical parameters used to represent the rock mass characteristics and D is the disturbance factor (slope excavation method) ranging from 0 (undisturbed *in situ* rock masses) to 1 (disturbed rock masses).

Table 2. *In situ* geotechnical properties obtained through field survey and laboratory tests for calculating $\text{RMR}_{\text{basic}}$ (after Bieniawski[5]), slope mass rating (SMR) (after Romana[7]) and geological strength index (GSI) (after Sonmez and Ulusay[10])

Parameters and their ratings	
UCS (MPa)	43.09
Rating	4
RQD%	72.5
Rating	13
Average joint spacing (m)	0.16
Rating	8
Joints condition	Slickenside surfaces
Rating	10
Groundwater conditions	Dripping
Rating	4
$\text{RMR}_{\text{basic}}$	39
F_1 adjustment ratings	0.70
F_2 adjustment ratings	1
F_3 adjustment ratings	–50
F_4 adjustment ratings	0
SMR	19
Volumetric joint count (J_v)	15
Structure rating (SR)	32.41
Roughness rating (R_r)	Smooth
Rating	1
Weathering rating (R_w)	Highly weathered
Rating	1
Infilling rating (R_i)	Soft <5 mm
Rating	2
Surface condition rating (SCR)	4
GSI	27

In this study, we also incorporated the pore water pressure (R_u) coefficient to simulate different water saturation conditions by assuming constant moisture levels at different depths. The obtained FoS values were 0.75, 0.71 and 0.69 for dry static, pseudo-static and wet conditions respectively (Figure 6 *c*) and thereby supporting a precarious slope.

This study describes the causative factors and failure mechanism responsible for triggering the Birik Dara landslide and also analyses the stability of the slope using diverse methods. A side-by-side comparison of the applied rock mass classification techniques, including kinematic analysis, reveals that the slope section is critically unstable, which has been further strengthened by FEM analysis (FoS ≤ 1). Although this landslide does not pose any direct risk to the settlements, it has a strong propensity to damage NH-10 and may affect the traffic. After the 2021 incident, the road was cleared for transportation, but it may be damaged again due to future rainfall/earthquake events. Considering the strategic significance of NH-10 as the only route for the people of Sikkim and Kalimpong to connect with the rest of India, it is imperative to develop appropriate stability measures to avoid future disastrous situations. The rationale behind this study is to ensure safe operation in this area, and also provide guidance to the decision-makers for landslide hazard mitigation and environmental remediation.

1. Cruden, D. and Varnes, D., Landslide types and processes. In *Landslides: Investigation and Mitigation. Special Report 247*, National Research Council. Transportation Research Board, Washington, DC, USA, 1996.
2. Acharyya, S. K., Structural framework and tectonic evolution of the eastern Himalaya. *Himalayan Geol*., 1980, **10**, 412–439.
3. Goel, R. K. and Subhash, M., Importance of weathering in rock engineering. In International Conference on Engineering Geology in New Millennium, Indian Institute of Technology Delhi, New Delhi, 2015, pp. 231–245.
4. Hoek, E. and Bray, J. D., *Rock Slope Engineering*, CRC Press, 1981, pp. 36–38.
5. Bieniawski, Z. T., The geomechanics classification in rock engineering applications. In 4th ISRM Congress, Onepetro, 1979.
6. Palmstrom, A., Measurements of and correlations between block size and rock quality designation (RQD). *Tunnel. Underg. Space Technol*., 2005, **20**(4), 362–377.
7. Romana, M., New adjustment ratings for application of Bieniawski classification to slopes. In Proceedings of the International Symposium on Role of Rock Mechanics, Zacatecas, Mexico, 1985, pp. 49–53.
8. Sarkar, S., Pandit, K., Sharma, M. and Pippal, A., Risk assessment and stability analysis of a recent landslide at Vishnuprayag on the Rishikesh–Badrinath highway, Uttarakhand, India. *Curr. Sci*., 2018, **114**(7), 1527–1533.
9. Hoek, E. and Brown, E. T., Practical estimates of rock mass strength. *Int. J. Rock. Mech. Min*., 1997, **34**(8), 1165–1186.
10. Sonmez, H. and Ulusay, R., A discussion on the Hoek–Brown failure criterion and suggested modifications to the criterion verified by slope stability case studies. *Yerbilimleri*, 2002, **26**, 77–99.
11. Das, S., Sarkar, S. and Kanungo, D. P., GIS-based landslide susceptibility zonation mapping using the analytic hierarchy process (AHP) method in parts of Kalimpong Region of Darjeeling Himalaya. *Environ. Monit. Assess*., 2022, **194**(3), 1–28.

ACKNOWLEDGEMENTS. S.D. thanks Sushanta Biswas for his support during field survey and the TLD-IV PS administrators for providing rainfall data. We thank the Director, CSIR-Central Building Research Institute, Roorkee for permission to publish this work. S.D. also thanks the University Grants Commission, New Delhi for the Junior Research Fellowship (JRF) (UGC-Ref. No. 3511/(NET-JULY 2018)) and the Academy of Scientific and Innovative Research, Ghaziabad for providing an opportunity to carry out this doctoral research.

Received 20 December 2021; revised accepted 27 July 2022

doi: 10.18520/cs/v123/i7/928-933

Preliminary observations on computerized tomography-powered fractal dimension-based technique to differentiate between coprolites and body fossils

Shubhabrata Sarkar[1], Sanjukta Chakravorti[2,3,*], Sudhir Kumar Chaudhary[1], Dhurjati P. Sengupta[2], Pankaj Wahi[1] and Prabhat Munshi[1]

[1]Nuclear Engineering and Technology Programme, Indian Institute of Technology Kanpur, Kanpur 208 016, India
[2]Geological Studies Unit, Indian Statistical Institute, 203, Barrackpore Trunk Road, Kolkata 700 108, India
[3]Department of Earth Sciences and Remote Sensing, JIS University, 81 Nilgunj Road, Kolkata 700 109, India

This study presents a fossil signature based on fractal dimension (FD) derived from computerized tomography (CT) images to differentiate between coprolites and body fossils. Coprolites are generally studied using destructive techniques like thin section study and geochemistry. Coprolites and body fossils collected from the Triassic terrestrial Gondwana deposits of India were chosen for the study. The presented CT-powered FD-based digital signature can properly distinguish coprolites from other fossils, without losing the structural features of the samples. The present study will further enhance the digitalized fossil research.

Keywords: Computerized tomography, coprolites, fossils, fractal dimension, X-ray.

LITHIFIED fossil faeces (coprolites) are highly variable trace fossils (records of behaviour of organisms preserved in rocks). They pose an analytical challenge for palaeontologists owing to their variable texture and shape. The study of coprolites is important as they reflect upon the dietary

*For correspondence. (e-mail: chirpymoni2009@gmail.com)